Substituent Effects on Charge Transport in Films of Au Nanocrystals

Gemma L. Stansfield and P. John Thomas*,[†]

School of Chemistry, Oxford Road, The University of Manchester, Manchester M139PL, U.K.

S *Supporting Information*

ABSTRACT: Charge transport (CT) in films of arylthiol-capped Au nanocrystals (NCs) exhibits strong substituent effects, with electron-donating substituents markedly decreasing conductivity. Films suited for measurements were obtained by ligand-exchange reactions on AuNCs grown at the water/toluene interface. Detailed analysis suggests the NCs interact with the ligands by resonance rather than inductive effects. The films were characterized by TEM, SEM, XPS, UV/vis, and AFM. CT characteristics were studied between 15 and 300 K.

Solids made of inorganic nanocrystals (NCs) sheathed by organic ligands are useful building blocks for opto-electronic devices, e.g., nanolasers and solar cells,[1] chemical[2] and biological[3] sensors, and plasmonic devices.[4] Much of their appeal is due to the profound changes to electronic, optical, and thermodynamic properties accompanying the acquisition of nanoscopic dimensions by the inorganic crystallites.[1,5,6] Our efforts to exploit the ensuing benefits are limited by surface ligands that present a strong barrier for movement of charges across NC solids. Ligands with long hydrocarbon chains commonly present in these solids are particularly effective at stifling charge transport (CT). Exchange with shorter bifunctional cross-linking ligands produces markedly improved conductivity (σ); e.g., an 8-fold increase in σ was obtained when the chain length was decreased from 9 methyl units to 3.[7] Particularly robust and conductive arrays of NCs were obtained using metal chalcogenide complex cross-linkers featuring ions such as $Sn_2S_6^{4-}$.[8]

Another paradigm is to employ single-tether (monofunctional) non-cross-linking ligands for better CT. Such ligands are potentially compatible with a wider variety of target NCs, are easier to synthesize, and feature easier exchange chemistry, yet they are rarely studied, as non-cross-linked films are mechanically less stable and reliable results are difficult to obtain. The potency of this method was recently illustrated by Nakanishi et al., who showed the photoconductivity of AuNC films can be switched from normal to inverse by simply changing the end functional groups of single-tether surface ligands.[9] Here, we find AuNCs grown at the water/toluene interface yield films of sufficient quality to permit what may be the first solid-state measurement of the effect of substituents on the CT characteristics of nanocrystalline films. Underpinning this study are the growth of AuNC films using molecular precursors *at* the water/toluene interface, faithful transfer of the film from the interface to a substrate, and labile phosphinyl surface ligands that can be easily replaced with a family of para-substituted thiophenols.

The film at the interface is a 3D superstructure made of dense aggregates of spheroidal clusters with diameters of several tens of nanometers. Each of these clusters is made of spherical NCs with diameters ~10 nm. Scanning electron microscopy (SEM) of films produced at 50 °C after 180 min shows a uniform and continuous deposit spanning many millimeters. Atomic force microscopy (AFM) and high-resolution SEM reveal irregular clusters with diameters ~70 nm (Supporting Information (SI), Figure S3; AFM shows these clusters are aggregates of spherical particulates. Transmission electron microscopy (TEM) of dispersions created by ultrasonically agitating the films reveals NCs with diameters ~10 nm (SI); the tendency of the AuNCs to aggregate, forming rafts with uniform interparticle spacing, is apparent. At shorter growth times (45 min), thinner, more fragile films suited for direct TEM imaging were obtained. The images reveal a dense monolayer of NCs with uniform separation distances. In interfacial films, the diameters of the NCs are not very uniform, nor is the structural order comparable to self-assembled arrays. Nevertheless, it is possible to repeatedly produce films (extending to areas of several mm^2) with identical CT characteristics using this technique, particularly when longer growth periods are employed. This unusual feature is accounted for, at least in part, by the the uniform interparticle separation distances seen in the TEM images. The films obtained after 180 min consist of ~10 layers of nanoparticles and are ~100 nm thick. The AuNCs in the films are capped with triphenylphosphine, tris(hydroxymethyl)phosphine, and other phosphine-based ligands.[10] The presence of these ligands was confirmed by X-ray photoelectron (XPS) and IR spectroscopy.[11] Our results on the structure and composition of these films agree well with previous studies on AuNC layers grown at the water/toluene interface.[10]

NCs with irregular surface structure consisting of labile ligands lack robust interparticle repulsion and would normally be incapable of forming extended structures.[6,12] Here, super-structure formation at the water/toluene interface is actively aided by the medium.[13] Assembly is initiated by adsorption of suitably capped NCs at the liquid/liquid interface. The initial adlayer reduces interfacial tension and aids the growth of multilayer films at the water/toluene interface. Note that it is necessary to adopt the facile transfer process described in the SI to relocate the interfacial superstructure onto solid substrates with minimal disruption and obtain films with uniform electronic properties. Soaking the films thus obtained in ethanolic solutions of thiophenol and its para-substituted derivatives results in replacement of phosphinyl ligands with

arylthiols. XPS on films before and after thiol derivatization indicates the P(2p) peak present initially is replaced by S(2p) features. In arylthiol-capped films, the Au:S ratios indicate 0.27−0.31 thiolate species per surface Au atom. This ratio is lower than typically seen on curved surfaces, where saturation coverage is expected to yield 0.40 thiolate/Au atom for spherical NCs with 10 nm diameter. We believe thiophenol forms a slightly disordered surface layer with less than saturation coverage. The propensity of thiophenol and it derivatives to form such a monolayer on flat Au substrates was previously reported.[14] TEM and SEM on interfacial films reveal no discernible changes to the structure after replacement of the surface ligands (Figure 1). Optical measurements (see below) support these observations.
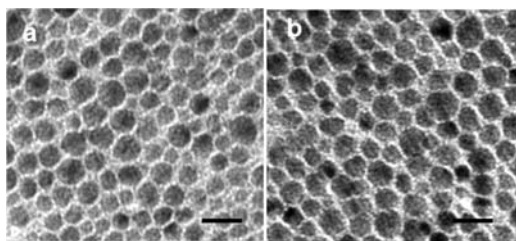

Figure 1. TEM images of AuNC films derivatized with (a) *p*-nitro- and (b) *p*-methoxythiophenol. Growth time, 45 min; scale bar, 20 nm.

To carry out reproducible CT measurements, the thickness and room temperature (RT) resistances of the as-prepared films were screened. Films with thickness of 100 ± 10 nm and resistance within 5% of the reported value were chosen. A majority of the as-prepared films satisfied this criteria. The σ values of arylthiol-coated AuNC films reveal clear nonmetallic behavior with a negative temperature coefficient throughout (Figure 2). Overall, σ decreases by ∼10% as the films are cooled from RT to 15 K. Such behavior akin to semiconductors is typical in films consisting of metal NC islands interspersed by long to medium-length organic ligands.[7,15,16] σ follows a model of activated hopping proposed by Neugebauer and Webb,[17]
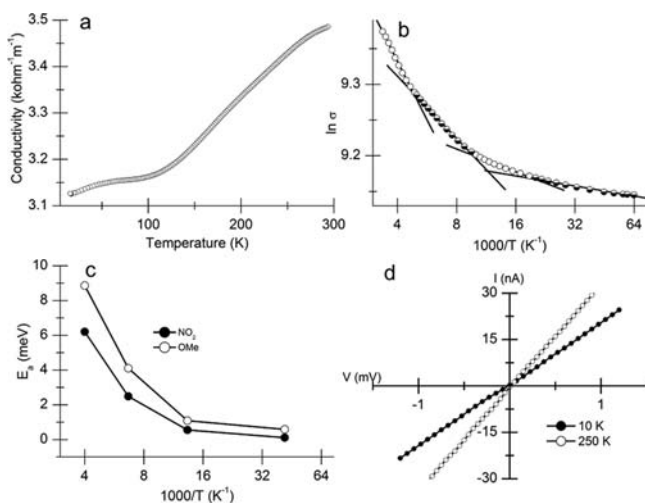
$$\sigma \propto e^{-2\delta\beta} \, e^{-E_a/kT} \tag{1}$$

where δ is the separation between the NCs, β the constant associated with tunneling between the NCs separated by a dielectric medium, and E_a the activation energy for electron-hopping between NCs. For NCs with a defined organic surface layer, δ and β may be assumed to be constant at various temperatures T (neglecting thermal expansion), giving

$$\sigma = A \, e^{-E_a/kT} \tag{2}$$

The activation energy is given by

$$E_a = \frac{1}{4\pi\varepsilon_0\varepsilon_r} \frac{e^2}{r} \tag{3}$$

where ε_0 is the vacuum permittivity, ε_r the dielectric constant of the medium surrounding the NCs, and r the radius of the NCs. E_a has also been defined via Coulomb energy expression[18] and more sophisticated formulations based on Marcus theory.[19] Regardless of the model used for E_a, substituents are expected to affect both E_a and A in (2).

Analysis of transport data reveals 4 distinct regimes of σ in arylthiol-capped Au films (Figure 2). Transitions between regimes are centered at $T \approx 200$, 100, and 50 K. In each of these domains, plots of $\ln \sigma$ vs $1/T$ are linear, suggesting the classical Arrhenius-type activated transport mechanism in (2) adequately describes the transport characteristics across the T range studied. Further, linear (ohmic) $I-V$ curves were obtained at various T, reinforcing the applicability of the activated hopping model (Figure 2b). In each of these regimes, a different mechanism of conductivity operates in the films.[7,16] Typically, as T is lowered, E_a falls in steps to <10 meV at the lowest T regime. At the same time, there is a relative increase in A, signaling a shift from hopping-dominated conduction mechanism to a tunneling-dominated one. However, activated hopping persists even at low T. Other studies on disordered metal NC films report a switch to variable-range hopping or tunneling mode of conductivity at low T since cooling causes localization of charge carriers.[20] Here, larger AuNCs, strong interparticle coupling, and regular interparticle spacing effectively overcome the localization effect.

Striking changes to the absolute conductivity of the films are seen (Figure 3) when different substituents are employed. Thiophenols bearing electron-donating substituents (methyl
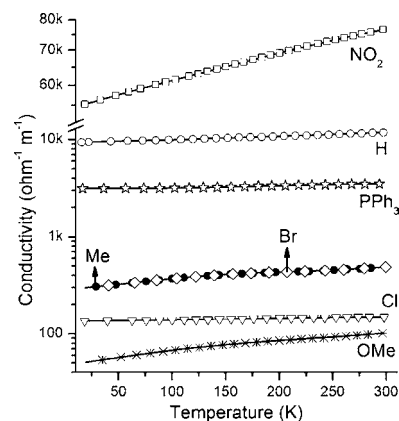

Figure 2. (a) σ vs T for thiophenol-coated AuNC films. (b) $\ln \sigma$ vs $1/T$; straight-line fits to the different σ regimes are shown. (c) E_a vs $1/T$; substituents are indicated. (d) $I-V$ curves for 4-methylthiophenol-coated AuNC films at 250 and 10 K.

Figure 3. Substituent effects on the conductivity of AuNC films. Functional groups at the para position of the thiophenol coating are shown. PPh$_3$ indicates phosphinyl ligands.

and methoxy in the para position) cause large decreases in σ relative to thiophenol-capped films; e.g., 4-methoxythiophenol reduces the RT σ value from 10 000 to 100 $\Omega^{-1}\,m^{-1}$, while the electron-withdrawing nitro substituent causes a sizable increase of σ from 10 000 to 75 000 $\Omega^{-1}\,m^{-1}$. Different substituents produce σ changes spanning 3 orders of magnitude. Br- and Cl-substituted thiophenols act akin to electron-donating groups rather than electron-withdrawing substituents and reduce σ. Remarkably, the T profiles of different films, which are highly sensitive to changes in morphology and structure,[1,5,6] are identical in that 4 nearly matching linear regimes can be identified in each case. These films seem to have a robust structure not particularly affected by the thiols employed.

The plasmon resonance band of the as-prepared AuNC films exhibits a large red-shift compared to NCs in solution (~530 nm), centered at ~705 nm.[21] The intensity and position of the peak exhibit clear substituent effects after ligand exchange (SI Figure S4). Exchange of the phosphinyl moiety with 4-nitrothiophenol results in a red-shift of the peak by ~20 nm; small changes to peak width and intensity are also seen. In contrast, 4-methoxythiophenol and other thiophenols strongly dampen the peak, causing ~50% intensity loss. Red-shifts indicate increased interaction between particles (or enhanced conductivity).[22] Dampening of peak intensity may be due to a reduction in the number of carriers forming the plasmon. In effect, changes to σ at RT are mirrored in the electronic absorption spectrum.

The effect of thiophenol substituents on conductivity can be accounted for using the dual-substituent parameter equation,

$$\log k = \rho_I \sigma_I + \rho_R \sigma_R^o + h \tag{4}$$

where k is the rate constant (replaced here by conductivity), σ_I and σ_R are constants corresponding to the inductive and resonance effects of the ligand, ρ_I and ρ_R represent the corresponding reaction constants, and h is a constant.[23] Electrostatic characteristics of a molecule, e.g., dipole moment, are captured by σ_I, while σ_R represents the ability of a molecule to delocalize charges. σ values sampled at 250, 150, 75, and 25 K, roughly corresponding to the midpoints of the 4 regimes of conductivity, were fitted to (4) by least-squares analysis to obtain the reaction constants and h; in each case correlations ≥ 0.94 were obtained (Figure 4). Significantly, the ρ values are positive, suggesting the reaction center is negatively charged in the transition state of the rate-determining step. If one assumes electrons are charge carriers and carrier transport occurs via a series of redox reactions, oxidation of negatively charged AuNCs is the slowest step. These observations strongly
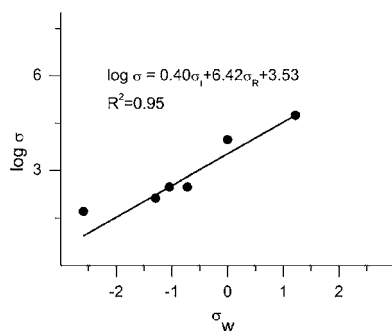

Figure 4. Correlation of substituent characteristics to σ of the films. Here, $\sigma_w = \rho_I \sigma_I + \rho_R \sigma_R^o$; see text for details.

contrast previous studies that regularly yielded the equivalent of negative ρ values.[24,25] Further, high values for the ratio ρ_R/ρ_I (the blending factor) suggest the ligands couple by resonance to the NCs. A classic test to confirm the nature of interaction is to move the substituents to the meta position, where overlap by resonance is not possible. Halo-substituted thiophenols would be expected to increase rather than decrease σ if moved to the meta position; we find this is indeed the case. The σ value of 3-chlorothiophenol-derivatized films increases (at RT) to 26 600 $\Omega^{-1}\,m^{-1}$, in contrast to the 4-chlorothiophenol-derivatized films, where σ falls to 150 $\Omega^{-1}\,m^{-1}$ (Figure 5).
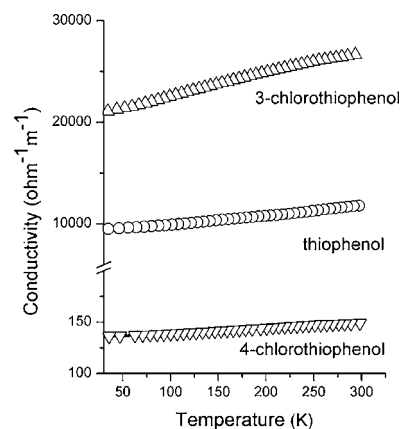

Figure 5. Changes to the transport characteristics of nanocrystalline films derivatized with p- and m-Cl-substituted thiophenols.

In simple terms, electron-withdrawing substituents provide additional area for delocalization for the Au species in the transition state, aiding CT, while electron-donating substituents localize the charge, hindering charge flow. Leaking of electron density from Au surfaces indicated in theoretical calculations may explain this substituent effect.[26] It is difficult to visualize through-bond resonance between metallic AuNCs and substituted thiophenols, but the evidence in terms of the effect of halogenated substituents, shifts in the electronic spectrum, and correlation to dual-substituent parameter equation seems unambiguous. Bredas et al., based on detailed calculations, proposed 2 conditions for the observation of strong molecular effects (including resonance effects) on Au surfaces: a surface monolayer with high rather than saturation coverage and the presence of subsituents no farther than the first phenyl ring.[27] Our experiment satisfies both conditions. Clearly, more attention must be paid to molecular topology in future studies of substituent effects on electronic properties of metal and semiconductor surfaces.

Murray et al. pioneered investigation of substituent effects on the ligand exchange rate and redox properties of well-defined AuNCs with Au_{38} core and found direct Hammett correlations to the substituent effects, with inductive effects dominating the NC/ligand interactions.[25] Similar results were obtained with Au_{25} core NCs.[28] It appears the larger metallic AuNCs studied here prefer to interact in a contrasting manner to their smaller, nonmetallic counterparts.

A critique of the analysis methodology may be in order. The dual-substituent parameter equation and related linear free energy relationships seek to explain the effect of substituents on rate constants for reactions carried out in liquid and gas phases. Application of such models to more complex solid-state reactions featuring multiple ligands per reacting entity is *per*

se not warranted. However, as shown by others[25,28] and here by us, meaningful correlations can indeed be obtained. Previously it was suggested that explanations based on electrostatic parameters such as dipole moments would also be apt, but no simple electrostatic explanation can account for the dominant resonance effects in the NC/ligand interaction observed here. The strong correlation may be insufficient to establish a direct resonant interaction between the particulates and the ligands. We believe this study suggests the NC/ligand interactions are more nuanced than previously suspected.

In summary, films of AuNCs capped with thiophenols exhibit strong substituent effects. The films' conductivity can be tuned between 100 and 75 000 $\Omega^{-1}\,m^{-1}$ by varying the substituent at the para position of the thiophenol capping ligands. Surprisingly, our analysis suggests a resonance effect dominates the interaction between NCs and ligands. This conclusion is generic and widely applicable across the whole body of NC solids. It would be of interest to see if this interaction is dependent on the diameters of the AuNCs. We envisage future research to test this hypothesis more extensively. Further, our synthetic scheme yields a robust set of nanoscopic electrodes suited for studies of the properties of molecules. We are presently carrying out detailed studies on these and other metal NC films grown at the interface.

■ ASSOCIATED CONTENT

Ⓢ Supporting Information

Experimental details, structural characteristics, absorption spectra, XPS, and analysis. This material is available free of charge via the Internet at http://pubs.acs.org.

■ AUTHOR INFORMATION

Corresponding Author

john.thomas@manchester.ac.uk or john.thomas@bangor.ac.uk

Present Address

[†]The School of Chemistry, Bangor University, Bangor, Gwynedd LL57 2UW, U.K.

Notes

The authors declare no competing financial interest.

■ ACKNOWLEDGMENTS

■ REFERENCES

(1) (a) Talapin, D. V.; Lee, J.-S.; Kovalenko, M. V.; Shevchenko, E. V. *Chem. Rev.* **2010**, *110*, 389. (b) Noginov, M. A.; Zhu, G.; Belgrave, A. M.; Bakker, R.; Shalaev, V. M.; Narimanov, E. E.; Stout, S.; Herz, E.; Suteewong, T.; Wiesner, U. *Nature* **2009**, *460*, 1110.

(2) (a) Cvelbar, U.; Mozetic, M. *J. Phys. D: Appl. Phys.* **2007**, *40*, 2300. (b) Huth, M. *J. Appl. Phys.* **2010**, *107*, 113709.

(3) Anker, J. N.; Hall, W. P.; Lyandres, O.; Shah, N. C.; Zhao, J.; Duyne, R. P. V. *Nature* **2008**, *7*, 442.

(4) Akimov, Y. A.; Koh, W. S.; Ostrikov, K. *Opt. Exp.* **2009**, *17*, 10195.

(5) Zabet-Khosousi, A.; Dhirani, A. *Chem. Rev.* **2008**, *108*, 4072.

(6) Rao, C. N. R.; Thomas, P. J.; Kulkarni, G. U. *Nanocrystals: Synthesis, Properties and Applications*; Springer-Verlag: Berlin, 2007.

(7) Pelka, J. B.; Brust, M.; Gierlowski, P.; Paszkowicz, W.; Schell, N. *Appl. Phys. Lett.* **2006**, *89*, 063110.

(8) Kovalenko, M.; Scheele, M.; Talapin, D. *Science* **2009**, *324*, 1417.

(9) Nakanishi, H.; Bishop, K. J. M.; Kowalczyk, B.; Nitzan, A.; Weiss, E. A.; Tretiakov, K. V.; Apodaca, M. M.; Klajn, R.; Stoddart, J. F.; Grzybowski, B. A. *Nature* **2009**, *460*, 371.

(10) (a) Sanyal, M. K.; Agrawal, V. V.; Bera, M. K.; Kalyanikutty, K. P.; Daillant, J.; Blot, C.; Kubowicz, S.; Konovalov, O.; Rao, C. N. R. *J. Phys. Chem. C* **2008**, *112*, 1729. (b) Luo, K.; Schroeder, S. L. M.; Dryfe, R. A. W. *Chem. Mater.* **2009**, *21*, 4172. (c) Rao, C. N. R.; Kulkarni, G. U.; Thomas, P. J.; Agrawal, V. V.; Saravanan, P. *J. Phys. Chem. B* **2003**, *107*, 7391. (d) Agrawal, V. V.; Kulkarni, G. U.; Rao, C. N. R. *J. Phys. Chem. B* **2005**, *109*, 7300.

(11) Stansfield, G. L.; Vanitha, P. V.; Johnston, H. M.; Fan, D.; AlQahtani, H.; Hague, L; Grell, M.; Thomas, P. J. *Philos. Trans. R. Soc. A* **2010**, *368*, 4313.

(12) Grzelczak, M.; Vermant, J.; Furst, E. M.; Liz-Marzán, L. M. *ACS Nano* **2010**, *4*, 3591.

(13) Niu, Z.; He, J.; Russell, T. P.; Wang, Q. *Angew. Chem., Int. Ed.* **2010**, *49*, 10052.

(14) Frey, S.; Stadler, V.; Heister, K.; Eck, W.; Zharnikov, M.; Grunze, M.; Zeysing, B.; Terfort, A. *Langmuir* **2001**, *17*, 2408.

(15) Joseph, Y.; Guse, B.; Vossmeyer, T.; Yasuda, A. *J. Phys. Chem. C* **2008**, *112*, 12507.

(16) Hardy, N. J.; Hanwell, M. D.; Richardson, T. H. *J. Mater. Sci.: Mater. Electron.* **2007**, *18*, 943.

(17) Neugebauer, C. A.; Webb, M. B. *J. Appl. Phys.* **1962**, *33*, 74.

(18) Andres, R. P.; Bielefield, J. D.; Janes, D. B.; Kolagunta, V. R.; Kubiak, C. P.; Mahoney, W. J.; Osifchin, R. G. *Science* **1996**, *273*, 1.

(19) Wuelfing, W. P.; Green, S. J.; Pietron, J. J.; Cliffel, D. E.; Murray, R. W. *J. Phys. Chem. C* **2008**, *112*, 12507.

(20) (a) Medeiros-Ribero, G.; Ohlberg, D. A. A.; Williams, R. S.; Heath, J. R. *Phys. Rev. B* **1999**, *59*, 1633. (b) Greshnykh, D.; Fromsdorf, A.; Weller, H.; Klinke, C. *Nano Lett.* **2009**, *9*, 473. (c) Liu, Y.; Gibbs, M.; Puthussery, J.; Gaik, S.; Ihly, R.; Hillhouse, H. W.; law, M. *Nano Lett.* **2010**, *10*, 1960. (d) Rao, C. N. R.; Kulkarni, G. U.; Agrawal, V. V.; Gautam, U. K.; Ghosh, M.; Tumurkar, U. *J. Colloid Interface Sci.* **2005**, *289*, 305. (e) Quinn, A. J.; Biancardo, M.; Floyd, L.; Belloni, M.; Ashton, P. R.; Preece, J. A.; Bignozzi, C. A.; Redmond, G. *J. Mater. Chem.* **2005**, *15*, 4403. (f) Talapin, D. V.; Murray, C. B. *Science* **2005**, *310*, 86. (g) Simon, U. *Adv. Mater.* **1998**, *10*, 1487. (h) Quinn, A. J.; Beecher, P.; Iacopino, D.; Floyd, L.; Marzi, G. D.; Shevchenko, E. V.; Weller, H.; Redmond, G. *Small* **2005**, *1*, 613.

(21) Agrawal, V. V.; Varghese, N.; Kulkarni, G. U.; Rao, C. N. R. *Langmuir* **2008**, *24*, 2494.

(22) Kreibig, U.; Vollmer, M. *Optical Properties of Metal Clusters*; Springer-Verlag: Berlin, 1995.

(23) (a) Taft, R. W.; Lewis, I. C. *J. Am. Chem. Soc.* **1958**, *80*, 2436. (b) Bromilow, J.; Brownlee, R. T. C.; Lopez, V. O.; Taft, R. W. *J. Org. Chem.* **1979**, *44*, 4766. (c) Isaacs, N. S. *Physical Organic Chemistry*; Longman Scientific and Technical: London, 1987.

(24) (a) Ashkenasy, G.; Cahen, D.; Cohen, R.; Shanzer, A.; Vilan, A. *Acc. Chem. Res.* **2002**, *35*, 121. (b) Kuo, C.-H.; Liu, C.-P.; Lee, S.-H.; Chang, H.-Y.; Lin, W.-C.; You, Y.-W.; Liao, H.-Y.; Shyue, J.-J. *Phys. Chem. Chem. Phys.* **2011**, *13*, 15122.

(25) (a) Guo, R.; Murray, R. W. *J. Am. Chem. Soc.* **2005**, *127*, 12140. (b) Guo, R.; Song, Y.; Wang, H.; Murray, R. W. *J. Am. Chem. Soc.* **2005**, *127*, 2752.

(26) Lang, N. D.; Kohn, W. *Phys. Rev. B* **1971**, *3*, 1215.

(27) Heimel, G.; Romaner, L.; Zojer, E.; Bredas, J.-L. *Acc. Chem. Res.* **2008**, *41*, 721.

(28) Parker, J. F.; Kacprzak, K. A.; Lopez-Acevedo, O.; Häkkinen, H.; Murray, R. W. *J. Phys. Chem. C* **2010**, *114*, 8276.

11891

dx.doi.org/10.1021/ja304348y | *J. Am. Chem. Soc.* 2012, 134, 11888–11891